Materials for Renewable and Sustainable Energy (2019) 8:2
https://doi.org/10.1007/s40243-018-0140-x

ORIGINAL PAPER

Structure and hydrogen storage properties of AB_3-type $Re_2Mg(Ni_{0.7-x}Co_{0.2}Mn_{0.1}Al_x)_9$ ($x=0-0.04$) alloys

L. Jiang[1] · Z. W. Zou[1] · Q. M. Pei[1] · D. S. Zheng[1] · F. S. Li[2] · Y. H. Tian[1]

Received: 24 September 2018 / Accepted: 10 December 2018 / Published online: 15 December 2018

Abstract

$Re_2Mg(Ni_{0.7-x}Co_{0.2}Mn_{0.1}Al_x)_9$ ($x=0-0.04$) alloys are prepared by induction melting, and the influence of the partial substitution of Ni by Al on the structure, hydrogen storage, and electrochemical properties of the alloys are investigated systematically. These alloys mainly consist of two main phases with $LaNi_5$ phase and $(La,Mg)_2Ni_7$ phase, and minor $LaNi_2$ phase. The pressure-composition isotherms shows that, with Al content increasing in the alloys, the maximum hydrogen storage capacity decreased from 1.16 wt% ($x=0$) to 0.99 wt% ($x=0.04$). The changes of enthalpy and entropy reveal that the thermodynamic stability and the disordered degree of the hydride alloys increase with the Al addition. Results of electrochemical studies indicate that the substitution of Al for Ni can noticeably improve the cycle stability of the alloy electrode. The capacity retention after 80 cycles is enhanced from 63.6% ($x=0$) to 76.5% ($x=0.04$). However, the maximum discharge capacity of the alloys decreases. The $Re_2Mg(Ni_{0.7-x}Co_{0.2}Mn_{0.1}Al_x)_9$ ($x=0-0.04$) alloys exhibit excellent dischargeability.

Keywords Metal hydride alloy · Thermodynamic enthalpy · Hydrogen storage property · Electrochemical characteristic

Introduction

Hydrogen storage alloys have attracted extensive attention because of their high energy storage density, long-charge/discharge cyclic life, and good environment compatibility properties [1, 2]. As the secondary Ni/MH batteries negative materials, the AB_5-type rare-earth-based hydrogen storage alloys and AB_2-type Zr-based or Ti-based alloys have been commercialized successfully [3]. However, the low capacity of AB_5-type alloys (the practical value is about 310 mAh g^{-1}) and the slow activation characteristics of AB_2-type alloys limit extensive applications [4–6]. Kadir et al. [7, 8] developed AB_3-type La–Mg–Ni alloys with $PuNi_3$ structure, which exhibited better characteristics than that of the conventional AB_5-type alloys. Not long after that, Kohno et al. [9] reported that the maximum discharge capacity of the $La_{0.7}Mg_{0.3}Ni_{2.8}Co_{0.5}$ alloy reached 410 mAh g^{-1}. Pan and his co-workers [10, 11] also acquired the similar results on the $La_{0.7}Mg_{0.3}(Ni_{0.85}Co_{0.15})_{3.5}$ alloy, namely with $PuNi_3$-type structure and the discharge capacity approaching 400 mAh g^{-1}, which exhibits good application prospect. The $PuNi_3$-type structure can be described as the growth along the c-axis of the alternate AB_2 and AB_5 subunit with 2:1 proportion [9]. Both AB_2 and AB_5 subunits can absorb hydrogen instead of only one AB_5 subunit. Moreover, magnesium hydrogen storage alloy is the most practical option due to its superiority in cost, weight, storage capacity, and material availability [12, 13]. Our previous research indicated that the ratio RE/Mg = 2 exhibited the best performance in $RE_{3-x}Mg_x(Ni_{0.7}Co_{0.2}Mn_{0.1})_9$ alloys [14]. Mg incorporation improved the discharge capacity of La–Mg–Ni-based alloys, and hence, this type alloy electrode become more and more attractive [15].

It is well known that elemental substitution is one of the most effective methods for improving the overall properties of hydrogen storage alloys. The substitution of rare-earth element at A site in La–Mg–Ni-type alloys can improve the electrode properties with a better anti-corrosion, as well as reducing the cost for commercial application. Zhang et al. [16, 17] pointed out that the La–Mg–Ni system alloy exhibited a improved cycle lifetime due to the significant corrosion decreasing caused by the appropriate

✉ L. Jiang
jiang2014long@163.com

[1] School of Physics and Optoelectronic Engineering, Yangtze University, Jingzhou 434023, People's Republic of China

[2] Chemical Functional Materials Research Center, Qujing Normal University, Qujing 655011, People's Republic of China

substitution of Ce for La. Zhai et al. [18, 19]. revealed that the cycle stability and the high-rate dischargeability of the $La_{1-x}Pr_xMgNi_{3.6}Co_{0.4}$ ($x = 0$–0.4) alloys obviously augmented with increasing Pr content. Ma et al. [20, 21] found that the electrochemical kinetics of the La–Mg–Ni-based hydrogen storage alloys could be effectively improved by partial substitution of Nd for La. Among them, praseodymium element is of great importance for cycle life of rare-earth-based hydrogen storage alloy electrodes.

Moreover, many meaningful research results at B site in the La–Mg–Ni system hydrogen storage alloys have also been done during recent years. Our previous research showed that suitable Mn content could effectively improve the discharge capacity and kinetics performance of hydrogen storage alloys [22]. The substitution of Ni by Mn noticeably decreased the stability of the hydrides against amorphisation on hydrogenation due to the change in crystal-structure type from $PuNi_3$ to $CeNi_3$ [23]. Many efforts have been made to improve the cycling stability of the La–Mg–Ni-base alloys by partial substitution Co for Ni, while the high-rate dischargeability needs to be further improved [24–26].

The Al substitution at B site is generally believed to be one of the most effective methods to improve the anti-corrosion ability of La–Mg–Ni-based alloys. Liao et al. [27] reported that Al incorporation decreased the discharge capacity and the high-rate dischargeability, but leads to a significant improvement the cycling stability of the electrode. Liu et al. [28] found that, with the addition of Al, the capacity cycling retention improved markedly due to the alleviated pulverization together with the Al oxide layer on the alloy surface during charge/discharge cycles. Annealing treatment technique promoted the AB_5 phase over the A_2B_7 phase in the $La_{0.7}Mg_{0.3}Ni_{2.8}Co_{0.5-x}Al_x$ alloys, while the annealed samples decreased the gaseous phase hydrogen storage and electrochemical capacities [29]. Guzik et al. [30] revealed that the Al atoms occupied 12% of the 6 h site within the $LaNi_5$ slabs in the $La_{0.77}Mg_{0.23}Ni_{3.41}Al_{0.09}$ alloy, which absorbed hydrogen when exposed to 10 bar of H_2 gas at room temperature. These research results provide important and valuable methods in improving the cycle stability of La–Mg–Ni-based electrode. However, to the best of our knowledge, no detailed work into the evidence for the stability of hydride alloys, and the hydrogen absorption/desorption mechanisms of the alloy electrodes are not entirely clear. Much more deeply study should be done to gain a better understanding the properties correlated with the Al presence.

In this paper, a series of alloys with chemical composition $Re_2Mg(Ni_{0.7-x}Co_{0.2}Mn_{0.1}Al_x)_9$ ($x = 0$–0.04) (Re: La-rich mischmetal) are prepared. The effect of Al substituting for Ni on the phase structure, hydrogen storage, and electrochemical properties of the series alloys are studied.

Experimental

Bulk metals (La, Pr, Mg, Ni, Co, Mn, and Al) from Aladdin were used as raw materials. The purity of all starting metals was above 99.9 wt%. The as-cast alloys were prepared by induction levitation melting on a water-cooled copper under argon atmosphere according to the stoichiometric composition $Re_2Mg(Ni_{0.7-x}Co_{0.2}Mn_{0.1}Al_x)_9$ ($x = 0$–0.04), where Re denotes $La_{0.85}Pr_{0.15}$. The 10 wt% excess of Mg and 5 wt% of Mn over composition was needed to compensate for evaporative loss under preparation progress. The alloys were turned over and re-melted thrice to ensure good homogeneity. The obtained ingots were then mechanically crushed and ground into the fine powder of 200 mesh size for the next experimentation. The microstructures of the $Re_2Mg(Ni_{0.7-x}Co_{0.2}Mn_{0.1}Al_x)_9$ ($x = 0$–0.04) powers were characterized at room temperature, using a Rigaku D/Max 2500 V diffractometer with Cu Kα radiation and a graphite monochromator operated at 40 kV and 200 mA, scanned with the rate of 6° min^{-1} in the 2θ range of 20–80°. The lattice parameters and cell volumes were analyzed using software Jade 5.0.

In studying the hydrogen storage properties, the pressure–composition–isotherms (P–C–T) curves of the alloys were measured with an automatic Sieverts-type apparatus under the pressure range of 10^{-3}–20 atm at given temperature. About 1.2 g alloy powder with particle size below 200 mesh was used for the test. For activation, the alloy powder was loaded in the clean reaction tube and exposed to the hydrogen atmosphere at room temperature to get rid of the air. Hydriding was conducted under 20 atm H_2 pressure for several minutes, and subsequent dehydriding was carried out by evacuating and heating the hydrided powder up to 300 °C. After repeated the hydriding/dehydriding process for three times, the P–C–T data were collected.

The hydride electrodes were prepared by mixing 0.3 g alloy powder (200 mesh) with 1.2 g carbonyl nickel powder. The mixture was then cold-pressed under a pressure of 20 MPa into a pallet of 15 mm in diameter and 1 mm in thickness. The prepared pellet, together with a Ni strip soldered on the surface, was inserted into folded current collector Ni foam, and the rims of the wrapped pellet were firmly spot-welded to keep the electrochemical contact well between the pellet, Ni strip, and Ni foam. The electrodes were immersed in 6 M KOH solution for 24 h to keep wet thoroughly before the tests. Electrochemical measurements were performed at 303 K in a standard three-electrode open cell consisting of a working electrode (hydride electrode), a sintered $Ni(OH)_2$/NiOOH counter electrode with excess capacity, and a Hg/HgO reference electrode immersed in 6 M KOH electrolyte. The emphasis of these measurements was on the electrochemical

properties of the working electrode, and thus, the discharge capacity of the counter electrode was designed to be much higher than that of the hydride electrode. Electrochemical tests were carried out on DC-5 automatic battery testing instrument. Each electrode was charged at 100 mA g^{-1} for 5 h followed by a 15 min break, and then discharged at 60 mA g^{-1} to a cut-off cell voltage of − 0.5 V versus the Hg/HgO reference electrode.

The cycle stability of the alloy electrodes was conducted by the charge/discharge process after 80 cycles and the cycle life was defined as the following equation:

$$S_{80} = C_{80}/C_{\max} \times 100\%,$$

wherein C_{80} was the discharge capacity at the 80th charge/discharge cycles and $C_{\max}$ was the maximum discharge capacity of the alloy electrodes. To investigate the discharge voltage characteristic of the alloy electrodes, the measurements were conducted after the alloy electrode was first completely activated.

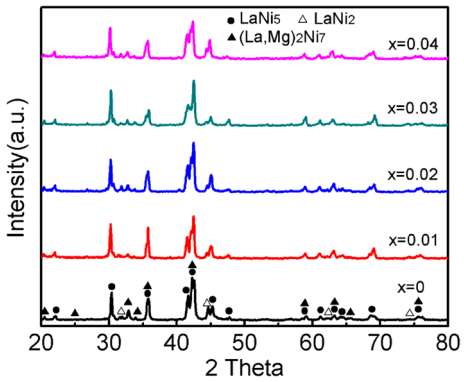

Fig. 1 X-ray diffraction patterns of the $Re_2Mg(Ni_{0.7-x}Co_{0.2}Mn_{0.1}Al_x)_9$ ($x = 0$–0.04)alloys

Results and discussion

Phase structure

Figure 1 shows the XRD patterns of the $Re_2Mg(Ni_{0.7-x}Co_{0.2}Mn_{0.1}Al_x)_9$ ($x = 0$–0.04) hydrogen storage alloys. It can be seen that the main phases in all of the alloys can be indexed as the characteristic peaks of the $LaNi_5$ phase with $CaCu_5$-type structure, and the $(La,Mg)_2Ni_7$ phase with Ce_2Ni_7-type structure, along with minor $LaNi_2$ phase with $MgCu_2$-type structure. The phase composition of the series alloys remains almost unchanged after partial substitution of Al for Ni. The similar results have been obtained in AB_3-type $La_2Mg(Ni_{1-x}Al_x)_9$($x = 0$–0.05) alloys [27]. That leads us to believe that Al atoms occupy the Ni site during substitution. The lattice parameter and the unit cell volume of all the phases in the alloys calculated by the Jade software are listed in Table 1. Owning to the fact that the atomic radius of Al (0.182 nm) is larger than that of Ni (0.162 nm), the parameters would be expected to be increased with the increasing x. However, the present results reveal that, with the progressively increasing substitution of Al for Ni in the alloys, both a parameters and c parameters of the $LaNi_5$ phase and the $LaNi_2$ phase increase, while a and c parameters of the $(La,Mg)_2Ni_7$ phase decrease.

To distinctly manifest the influence of Al on the lattice parameters of phases in the alloys, the cell volume dependence of Al content is plotted in Fig. 2. It can be seen that, with the increasing x, the cell volume of both $LaNi_5$ phase

Table 1 Crystal lattice parameter of $Re_2Mg(Ni_{0.7-x}Co_{0.2}Mn_{0.1}Al_x)_9$($x = 0$–$0.04$)alloys

Samples	Space group	Phase	Cell parameter		Cell volume/nm^3
			A/nm	*C*/nm	
$x = 0$	P6/mmm (191)	$LaNi_5$	0.5002 (2)	0.4002 (1)	0.0867
	$P6_3/mmc$ (194)	$(La,Mg)_2Ni_7$	0.4974 (2)	2.4603 (8)	0.5272
	Fd-3 m (227)	$LaNi_2$	0.7194 (1)	–	0.3723
$x = 0.01$	P6/mmm (191)	$LaNi_5$	0.5003 (4)	0.4011 (9)	0.0870
	$P6_3/mmc$ (194)	$(La,Mg)_2Ni_7$	0.4972 (5)	2.4591 (4)	0.5267
	Fd-3 m (227)	$LaNi_2$	0.7200 (4)	–	0.3733
$x = 0.02$	P6/mmm (191)	$LaNi_5$	0.5005 (5)	0.4019 (7)	0.0871
	$P6_3/mmc$ (194)	$(La,Mg)_2Ni_7$	0.4969 (8)	2.4575 (7)	0.5263
	Fd-3 m (227)	$LaNi_2$	0.7203 (3)	–	0.3739
$x = 0.03$	P6/mmm (191)	$LaNi_5$	0.5010 (6)	0.4023 (5)	0.0873
	$P6_3/mmc$ (194)	$(La,Mg)_2Ni_7$	0.4967 (8)	2.4565 (7)	0.5257
	Fd-3 m (227)	$LaNi_2$	0.7211 (2)	–	0.3749
$x = 0.04$	P6/mmm (191)	$LaNi_5$	0.5012 (3)	0.4028 (0)	0.0876
	$P6_3/mmc$ (194)	$(La,Mg)_2Ni_7$	0.4965 (1)	2.4556 (2)	0.5255
	Fd-3 m (227)	$LaNi_2$	0.7220 (4)	–	0.3764

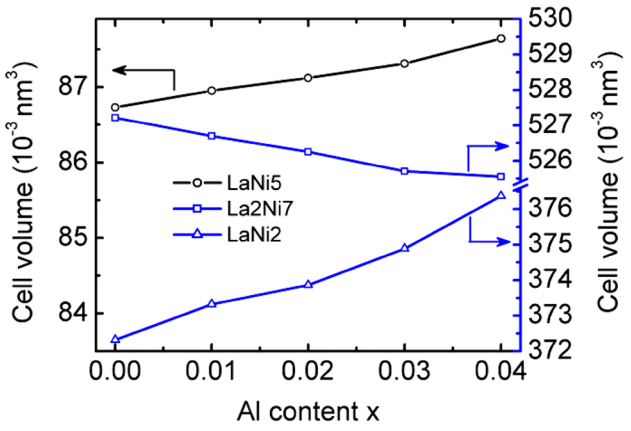

Fig. 2 Variation of cell volume in different phases of $Re_2Mg(Ni_{0.7-x}Co_{0.2}Mn_{0.1}Al_x)_9$($x=0$–$0.04$)alloys

and $LaNi_2$ phase in the alloys increases almost linearly, whereas the cell volume of $(La,Mg)_2Ni_7$ phase shrinks slightly. That means, the partial substitution of Al for Ni has only enlarged the structure of $LaNi_5$ phase and $LaNi_2$ phase in the $Re_2Mg(Ni_{0.7-x}Co_{0.2}Mn_{0.1}Al_x)_9$ ($x=0$–0.04) alloys. In La–Mg–Ni-based alloys, Al element tended to enter $LaNi_5$ phase rather than $(La,Mg)_2Ni_7$ phase during Al incorporation [28]. Obtained results reveal that Al atoms have a strong preference and tend to enter to the $LaNi_5$ and $LaNi_2$ structure. The slight shrinking of $(La,Mg)_2Ni_7$ phase is attributed to the lattice distortion during the Al substitution.

P–C– isotherms

To investigate the effect of Al content on the hydrogen absorption/desorption properties, the P–C–T curves of the $Re_2Mg(Ni_{0.7-x}Co_{0.2}Mn_{0.1}Al_x)_9$ ($x=0$–0.04) alloys at different temperatures are plotted in Fig. 3a–e. From these curves, the maximum hydrogen storage capacity (MH_{max}, under 20 atm) can be obtained, and the results measured at 303 K are also listed in Table 2. It can be seen that, at given temperature, MH_{max} of the $Re_2Mg(Ni_{0.7-x}Co_{0.2}Mn_{0.1}Al_x)_9$ ($x=0$–0.04) alloys goes down continually with the increasing x. For example, at 303 K, with the substitution of Al for Ni, MH_{max} of the $Re_2Mg(Ni_{0.7-x}Co_{0.2}Mn_{0.1}Al_x)_9$ alloys is 1.16, 1.10, 1.06, 1.04, and 0.99 wt% for $x=0$, 0.01, 0.02, 0.03, and 0.04, respectively. In La–Mg–Ni system alloys, the La_2Ni_7-type phase plays a dominant role in hydrogen storage capacity of the alloys [31]. The change of hydrogen storage capacity for $Re_2Mg(Ni_{0.7-x}Co_{0.2}Mn_{0.1}Al_x)_9$ alloys results from the relative variation of the phase abundance of the $(La, Mg)_2Ni_7$ phase and $LaNi_5$ phase [24].

The gaseous phase hydrogen storage properties of the $Re_2Mg(Ni_{0.7-x}Co_{0.2}Mn_{0.1}Al_x)_9$ alloys at 303 K are displayed in Fig. 4. It can be found that the slopes of P–C–T curves are very steep and there is almost no plateau in the absorption/desorption process during the substitution Al for Ni. There are three possible reasons which lead to the steep plateau: (1) A certain portion of the crystalline alloy changes to the amorphous state upon hydriding [27];(2) The loss of Mg volatilization during melting of the alloys also results in the steep plateau [32], which can be improved by adding excess Mg to the synthesis; (3) The alloys possess multi-phase structure, and the compounding of the differing absorption/desorption pressures of their components leads to the steep plateau [33]. In the present study, because the Mg content is excessive during melting, we think that the steep plateau is attributed to the above (1) or/and (3) reasons.

The plateau pressure shown in this work is defined as the mean of the mid-hydrogen storage capacity from the P–C–T curves. The relation between the composition and the plateau pressure of the $Re_2Mg(Ni_{0.7-x}Co_{0.2}Mn_{0.1}Al_x)_9$ ($x=0$–0.04) alloys can be obtained from Fig. 4, and is given in Table 2. As we all know, there is a hysteresis loop between hydrogen absorption and desorption due to the pressure discrepancy, which can be characterized by a hysteresis factor, calculated using $H_f=\ln(P_a/P_d)$, where P_a and P_d stand for the hydrogen absorption and desorption plateau pressure, respectively. As can be seen in Table 2, with the increasing Al content, H_f becomes larger, implying more energy loss happened during at least one of the absorption and desorption processes. Energy loss results in the increase of the irreversibility between hydrogen absorption and desorption. That is, the elevating portion of the hydrogen in the alloys cannot be released with the increasing Al content, which is consistent with the results reported in the literature [27]. This phenomenon is disadvantageous to the practice application. Moreover, H_f can also be used to predict the pulverization rate of the alloy during charge/discharge cycling [34]. The cycling stability will be discussed latter.

Thermodynamic property

To further understand the hydride properties of composites, the thermodynamics parameters for the hydrogenation of these composites are determined from Van't Hoff equation $\ln P=\Delta H/RT-\Delta S/T$. From the slope and intercept of Van't Hoff plot, as shown in Fig. 5, the enthalpy change ΔH is calculated to be −24.82, −26.47, −31.30, −34.76, and −36.49 kJ/mol H_2, and the entropy change ΔS is found to be −87.35, −94.23, −113.70, −128.02, and −137.02 J/mol H_2K for $x=0$, 0.01, 0.02, 0.03, and 0.04, respectively. These values are similar or comparable to the commercial AB_5 and AB_2 MH alloys [35, 36]. ΔH is very important for evaluating the utilization of hydrogen storage alloys. Metal hydride with larger ΔH absolute value needs higher temperature to desorb hydrogen, suggesting that the hydride is more stable [37]. Metal hydride with strong thermodynamic stability is believed to be detrimental to hydrogen desorption. In the

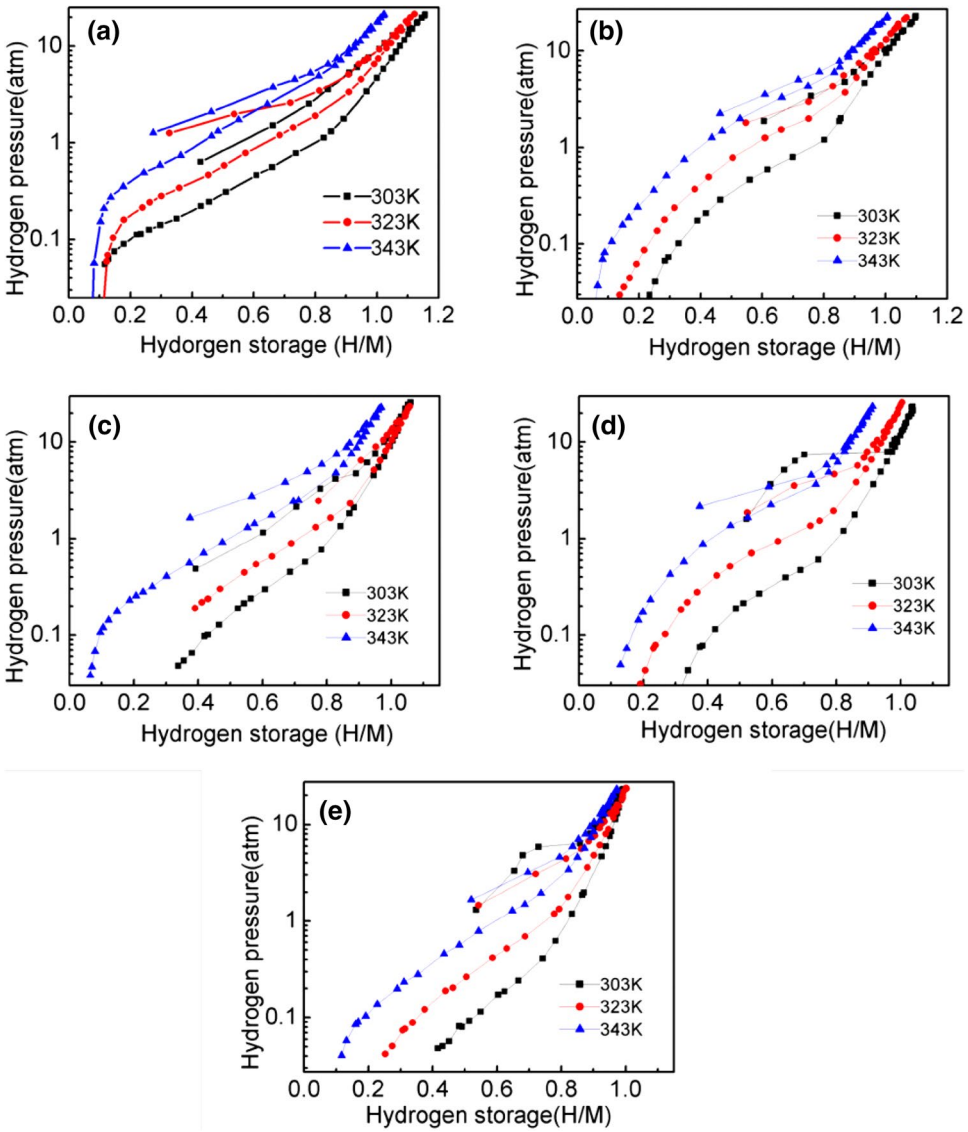

Fig. 3 P–C–T curves of $Re_2Mg(Ni_{0.7-x}Co_{0.2}Mn_{0.1}Al_x)_9$ ($x=0-0.04$)alloys at different temperature: **a** $x=0$, **b** $x=0.01$, **c** $x=0.02$, **d** $x=0.03$, and **e** $x=0.04$

Table 2 Hydrogen storage characters of the $Re_2Mg(Ni_{0.7-x}Co_{0.2}Mn_{0.1}Al_x)_9$ alloy (303 K)

Samples	MH_{max} (wt%)	Plateau pressure(atm)		Hysteresisfactor H_f	C_{max} (mAh g^{-1})	S_{80}(%)
		P_a	P_d			
$x=0$	1.16	1.51	0.46	0.51	328.7	63.6
$x=0.01$	1.10	1.88	0.46	0.61	322.2	65.4
$x=0.02$	1.06	1.15	0.21	0.73	321.7	70.6
$x=0.03$	1.04	1.58	0.21	0.87	317.0	71.5
$x=0.04$	0.99	1.31	0.08	1.21	312.7	76.5

present case, the absolute values of ΔH become markedly higher with increasing Al content, suggesting that the stability of the hydrides increases as Al is added. Hence, the dehydriding process becomes more difficult and the reversible hydrogen storage capacity decreases. This result is consistent with H_f mentioned above. The other parameter ΔS is used to describe the disorder degree of the hydride alloys; the larger $-\Delta S$ means that the hydride of the alloys is more obvious deviate to the perfect ordered structure, indicating that the filling of an ordered MH structure is not completed [36, 38]. Judging from the experimental data, $-\Delta S$ values of the alloys upgrade distinctly with the increase of Al content. We can deduce that the enhancing Al content causes an incompletion in the formation of a complete ordered metal

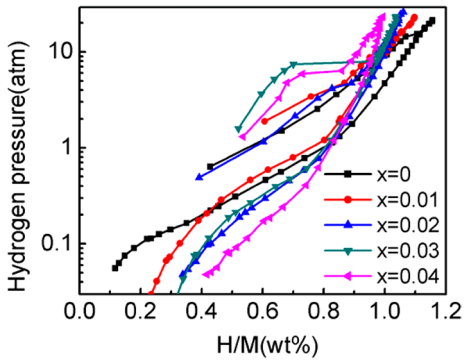

Fig. 4 P–C–T curves of the $Re_2Mg(Ni_{0.7-x}Co_{0.2}Mn_{0.1}Al_x)_9$ ($x=0$–0.04) alloys at 303 K

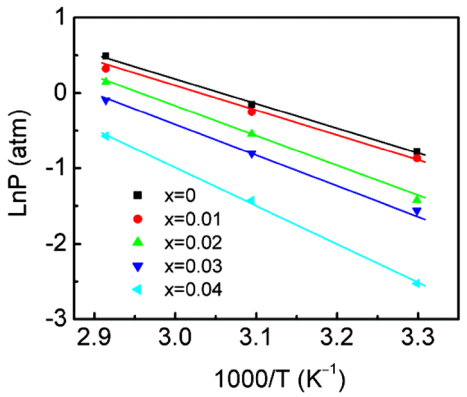

Fig. 5 Van't Hoff plots for hydrogen desorption of $Re_2Mg(Ni_{0.7-x}Co_{0.2}Mn_{0.1}Al_x)_9$($x=0$–$0.04$)alloys

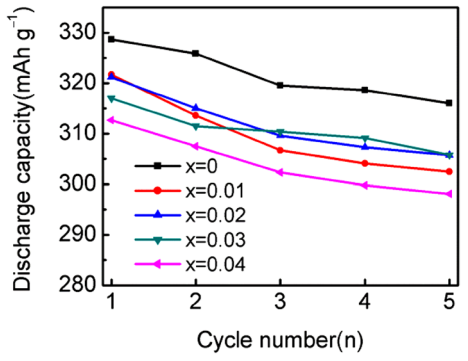

Fig. 6 Activation course the $Re_2Mg(Ni_{0.7-x}Co_{0.2}Mn_{0.1}Al_x)_9$ ($x=0$–0.04) electrode alloys

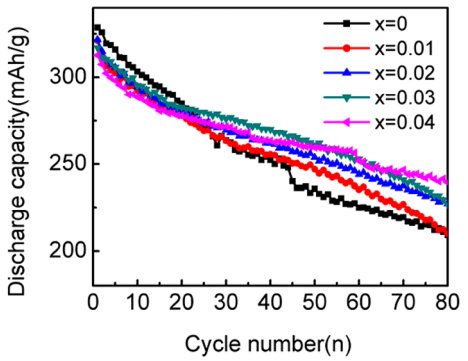

Fig. 7 Cycle life curves of the Re $_2Mg(Ni_{0.7-x}Co_{0.2}Mn_{0.1}Al_x)_9$ ($x=0$–0.04) alloys

hydride structure. Therefore, with increasing x, the disordered degree of the hydride alloys increases, which yields the lower hydrogen storage capacity.

Activation and cyclic stability

The activation performance and the maximum discharge capacities (C_{max}) of the electrodes are measured at the condition of the current density of 60 mA g^{-1}. Figure 6 illustrates the discharge capacities of $Re_2Mg(Ni_{0.7-x}Co_{0.2}Mn_{0.1}Al_x)_9$ ($x=0$–0.04) electrode alloys which vary with cycle numbers; C_{max} is also listed in Table 2. It is found that all of the investigated alloys can easily activate and reach the maximum discharge capacity at the initial charge/discharge process, which is favorable for their commercial application. No noticeable differences can be observed in the activation performance of these electrodes, which is attributed to the same multi-phase composition of these alloys [39]. Figure 6 also shows that, with increasing Al content, C_{max} of the alloys monotonously decreases from 328.7 mAh g^{-1} ($x=0$) to 312.7 mAh g^{-1} ($x=0.04$). Ni is well known as an indispensable element in hydrogen storage electrode alloys due to their high electrocatalytic [40]. The decline of C_{max} should be partly attributed to the reduced Ni content. Moreover, compared to Ni, Al has a smaller electronegativity, which leads to a relative smaller repulsion to the electron accompanying an adsorbed hydrogen atom. Similar results were obtained for the substitution of Mn for Ni [32]. Furthermore, it can be clearly seen that the changing trend of the discharge capacity is good agreement with that of the hydrogen storage capacity with substitution Al for Ni, verifying the charge/discharge progress in electrochemical reaction corresponding to the absorption/desorption progress in gas–solid reactions.

The cyclic stability of hydrogen storage alloy is a decisive factor for the Ni/MH batteries life, which directly relates to the practical applications. The discharge capacities of the $Re_2Mg(Ni_{0.7-x}Co_{0.2}Mn_{0.1}Al_x)_9$($x=0$–$0.04$)alloy electrodes as a function of cycle number are plotted in Fig. 7. The relative results are also summarized in Table 2. It can be seen that, with Al content increasing, the capacity retention (S_{80}) increases from 63.6% ($x=0$) to 76.5% ($x=0.04$) after 80 charge/discharge cycles, which indicates that the partial substitution of Al for Ni significantly improves the cycling stability of the alloy electrode. However, the present

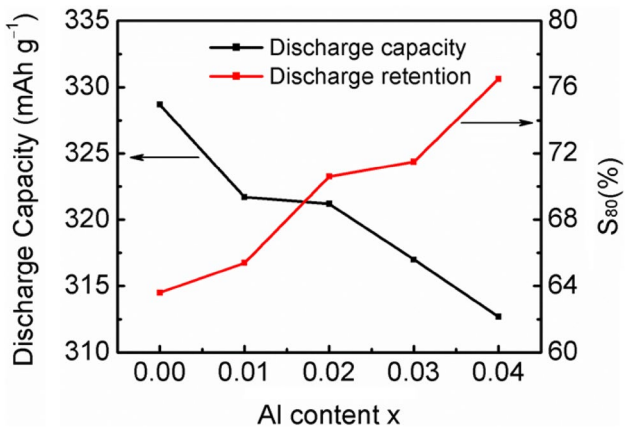

Fig. 8 Relationship between the capacity retention rate (S_{80}) and Al content (x) of the $Re_2Mg(Ni_{0.7-x}Co_{0.2}Mn_{0.1}Al_x)_9$ ($x=0$–0.04) alloys

result is poor compared with the results reported by Pan et al. [27] partly because of the existence of Mn element in these alloys.

The relationship between the discharge capacity, the cycle stability, and the Al content in the $Re_2Mg(Ni_{0.7-x}Co_{0.2}Mn_{0.1}Al_x)_9$($x=0$–$0.04$) electrode alloys is also plotted in Fig. 8. In the hydrogen storage alloys, there are two important factors responsible for the degradation of the discharge capacity of the alloy electrodes during charge/discharge cycles: [41, 42] the pulverization of the alloys particles and corrosion/oxidation of the active compositions. On one hand, the improvement of the stability of the alloy electrodes could ascribe to the higher pulverization resistance during cycling [43]. As discussed in P–C-isotherms, H_f raise with the increasing amount of Al substitution, the alloys with larger H_f possess higher rigidity, which lead to increase the anti-pulverization ability for the reduction of the capacity decline rate with cycling. On the other hand, it is well known that Al in alkaline solution is easily oxidized to Al oxide, which protects the alloy electrode from being further corroded/oxidized in KOH solution. Similar results [44, 45] have been reported that the addition of Al in La–Mg–Ni-based alloys can form a thicker oxide film, which effectively shields the alloy from being corroded on the surface contacting the electrolyte. The Al_2O_3 film can also prevent hydrogen diffusion from the surface to the bulk of alloys, so the kinetic properties of alloys were deteriorated. Therefore, the partial substitution of Al for Ni exhibits a more pronounced effect on the cycle life of the $Re_2Mg(Ni_{0.7-x}Co_{0.2}Mn_{0.1}Al_x)_9$ ($x=0$–0.04) alloys.

Discharge characteristic

The discharge voltage characteristic is an important performance of the electrode alloy, which is characterized by the potential plateau of the discharge curve of the alloy. The discharge potential plateau of alloy electrode corresponds to the oxidation process of desorbed hydrogen from metal hydride [46]. Thus, the better discharge characteristic of the alloys is determined by the longer and more horizontal discharge voltage plateau. Figure 9 shows the discharge curves of $Re_2Mg(Ni_{0.7-x}Co_{0.2}Mn_{0.1}Al_x)_9$ ($x=0$–0.04) alloy electrodes at 60 mA g^{-1} and 303 K after being activated. The discharge potential plateau is between 0.84 and 0.92 V. Obviously, each composite alloy electrode has a longer and horizontal potential plateau, and the $Re_2Mg(Ni_{0.7-x}Co_{0.2}Mn_{0.1}Al_x)_9$ ($x=0$–0.04) alloy electrodes exhibit almost the same discharge potential plateau, which can be attributed to the similar phase component. Moreover, during discharge process, the discharge plateau above 0.84 V maintains the discharge capacity over 90% of C_{max}, and then decreases sharply down below 0.84 V, indicating that alloy electrode possesses a high and stable discharge potential. The excellent discharge plateau may be ascribed to the multi-phase phase in the alloy, which increases the phase boundaries to provide more tunnels for the diffusion of hydrogen [47]. Therefore, the diminution of the diffusion resistance of the alloys leads to the high discharge potential.

Conclusions

The relationship of the structure, hydrogen storage and electrochemical performance for the $Re_2Mg(Ni_{0.7-x}Co_{0.2}Mn_{0.1}Al_x)_9$($x=0$–$0.04$) alloys has been investigated. Partial substitution of Al for Ni in metal hydride alloy induced the change of structural parameter. The substitution of Al for Ni of $Re_2Mg(Ni_{0.7-x}Co_{0.2}Mn_{0.1}Al_x)_9$ ($x=0$–0.04) alloys happened in $LaNi_5$ phase and $LaNi_2$ phase prior to $(La, Mg)_2Ni_7$ phase. With Al content increasing in the alloys, the hydrogen storage capacity decreased from 1.16 wt% ($x=0$) to 0.99 wt% ($x=0.04$) at 303 K. The increasing absolute value of

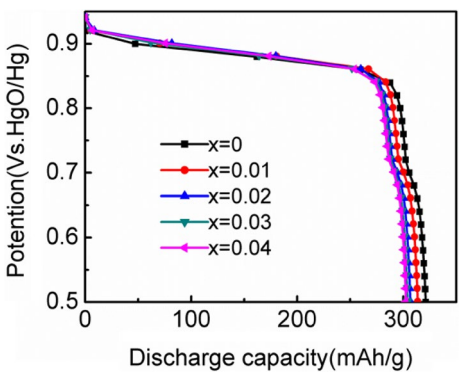

Fig. 9 Discharge voltage curves of the $Re_2Mg(Ni_{0.7-x}Co_{0.2}Mn_{0.1}Al_x)_9$ ($x=0$–0.04) alloys

enthalpy change ΔH from 24.82 to 36.49 kJ/mol and the entropy change ΔS from 87.35 to 137.02 J/mol revealed that the thermodynamic stability and disordered degree of the hydrides alloys increased with the Al addition. The discharge capacity of the alloys decreased with the increase of Al content, while the cycle stability (S_{80}) improved noticeably, increasing from 63.6% ($x=0$) to 76.5% ($x=0.04$). The $Re_2Mg(Ni_{0.7-x}Co_{0.2}Mn_{0.1}Al_x)_9$ ($x=0-0.04$) alloys have higher discharge potential above 0.84 V, exhibiting high and stable discharge plateau.

Acknowledgements This work was supported by the National Natural Science Foundation of China (No.11605014), the Natural Science Foundation of Hubei Province (No.2017CFB576), and Jingzhou Science and Technology Development Plan Project (No. 2016AD50-4).

References

1. Liu, Y.F., Cao, Y.H., Huang, L., Gao, M.X., Pan, H.G.: Rare earth-Mg–Ni-based hydrogen storage alloys as negative electrode materials for Ni/MH batteries. J. Alloy. Compd. **509**, 675–686 (2011)
2. Meena, P., Jangir, M., Singh, R., Sharma, V.K., Jain, I.P.: Synthesis and hydrogen storage of $La_{23}Nd_{7.8}Ti_{1.1}Ni_{33.9}Co_{32.9}Al_{0.65}$ alloys. J. Mater. Res. Technol. **7**(2), 173–179 (2018)
3. Feng, F., Geng, M., Northwood, D.O.: Electrochemical behaviour of intermetallic-based metal hydrides used in Ni/metal hydride (MH) batteries: a review. Int. J. Hydrog. Energy **26**, 725–734 (2001)
4. Li, Y., Lei, Y.Q., Chen, L.X., Lu, G.L., Wang, Q.D.: The structure and electrochemical properties of La2MgNix(x = 8.7–9.9) hydrogen storage electrode alloys. J. Alloy. Compd. **429**, 329–334 (2007)
5. Kim, D.M., Jang, K.J., Lee, J.Y.: A review on the development of AB_2-type Zr-based Laves phase hydrogen storage alloys for Ni–MH rechargeable batteries in the Korea Advanced Institute of Science and Technology. J. Alloy. Compd. **293–295**, 583–592 (1999)
6. Du, Y.L., Yang, X.G., Zhang, Q.A., Lei, Y.Q., Zhang, M.S.: Phase structures and electrochemical properties of the Laves phase hydrogen storage alloys $Zr_{1-x}Ti_x(Ni_{0.6}Mn_{0.3}V_{0.1}Cr_{0.05})_2$. Int. J. Hydrog. Energy **26**, 333–337 (2001)
7. Kadir, K., Sakai, T., Uehara, I.: Synthesis and structure determination of a new series of hydrogen storage alloys; RMg_2Ni_9 (R = La, Ce, Pr, Nd, Sm and Gd) built from $MgNi_2$ Laves-type layers alternating with AB_5 layers. J. Alloy. Compd. **257**, 115–121 (1997)
8. Kadir, K., Sakai, T., Uehara, I.: Structural investigation and hydrogen storage capacity of $LaMg_2Ni_9$ and $(La_{0.65}Ca_{0.35})(Mg_{1.32}Ca_{0.68})Ni_9$ of the AB_2C_9 type structure. J. Alloy. Compd. **302**, 112–117 (2000)
9. Kohno, T., Yoshida, H., Kawashima, F., Inaba, T., Sakai, I., Yamamoto, M., Kanda, M.: Hydrogen storage properties of new ternary system alloys: La_2MgNi_9, $La_5Mg_2Ni_{23}$, La_3MgNi_{14}. J Alloy. Compd. **311**, L5–L7 (2000)
10. Pan, H.G., Liu, Y.F., Gao, M.X., Lei, Y.Q., Wang, Q.D.: A study of the structural and electrochemical properties of $La_{0.7}Mg_{0.3}(Ni_{0.85}Co_{0.15})x$ (x = 2.5–5.0) hydrogen storage alloys. J. Electrochem. Soc. **150**, A565–A570 (2003)
11. Pan, H.G., Liu, Y.F., Gao, M.X., Zhu, Y.F., Lei, Y.Q., Wang, Q.D.: An investigation on the structural and electrochemical properties of $La_{0.7}Mg_{0.3}(Ni_{0.85}Co_{0.15})_x$ ($x=3.15–3.80$) hydrogen storage electrode alloys. J. Alloy. Compd. **351**, 228–234 (2003)
12. Jain, I.P., Lal, C., Jain, A.: Hydrogen storage in Mg: a most promising material. Int. J. Hydrog. Energy **35**, 5133–5144 (2010)
13. Meena, P., Singh, R., Sharma, V.K., Jain, I.P.: Role of $NiMn_{9.3}Al_{4.0}Co_{14.1}Fe_{3.6}$ alloy on dehydrogenation kinetics of MgH_2. J. Magn. Alloy. **6**, 318–325 (2018)
14. Jiang, L., Lan, Z.Q., Li, G.X., Guo, J.: Influence of magnesium on electrochemical properties of $RE_{3-x}Mgx(Ni_{0.7}Co_{0.2}Mn_{0.1})_9$(x = 0.5–1.25) alloy electrodes. J. Rare Earth **30**, 1255–1259 (2012)
15. Cao, J., Zhao, Y.M., Zhang, L., Jia, Z.R., Wang, W.F., Dong, Z.T., Han, S.M., Li, Y.: Effect and mechanism of Mg on crystal structures and electrochemical cyclic stability of Ce_2Ni_7-type La–Mg–Ni-based hydrogen storage alloys. Int. J. Hydrog. Energy **43**, 17800–17808 (2018)
16. Zhang, X.B., Sun, D.Z., Yin, W.Y., Chai, Y.J., Zhao, : Effect of La/Ce ratio on the structure and electrochemical characteristics of $La_{0.7-x}Ce_xMg_{0.3}Ni_{2.8}Co_{0.5}$($x=0.1–0.5$) hydrogen storage alloys. Electrochim. Acta **50**, 1957–1964 (2005)
17. Lv, W., Yuan, J.G., Zhang, B., Wu, Y.: Influence of the substitution Ce for La on structural and electrochemical characteristics of $La_{0.75-x}Ce_xMg_{0.25}Ni_3Co_{0.5}$ ($x=0$, 0.05, 0.1, 0.15, 0.2 at%) hydrogen storage alloys. J. Alloy. Compd. **730**, 360–368 (2018)
18. Zhai, T.T., Yang, T., Yuan, Z.M., Xu, S., Bu, W.G., Qi, Y., Zhang, Y.H.: Influences of hydrogen-induced amorphization and annealing treatment on gaseous hydrogen storage properties of $La_{1-x}Pr_xMgNi_{3.6}Co_{0.4}$ (x = 0–0.4) alloys. J. Alloy. Compd. **639**, 15–20 (2015)
19. Zhai, T.T., Yang, T., Yuan, Z.M., Zhang, Y.H.: An investigation on electrochemical and gaseous hydrogen storage performances of as-cast $La_{1-x}Pr_xMgNi_{3.6}CO_{0.4}$ (x = 0–0.4) alloys. Int. J. Hydrog. Energy **39**, 14282–14287 (2014)
20. Ma, S., Gao, M.X., Li, R., Pan, H.G., Lei, Y.Q.: A study on the structural and electrochemical properties of $La_{0.7-x}Nd_xMg_{0.3}Ni_{2.45}Co_{0.75}Mn_{0.1}Al_{0.2}$ (x = 0.0–3.0) hydrogen storage alloys. J. Alloy. Compd. **457**, 457–464 (2008)
21. Li, Y., Han, S.M., Li, J.H., Zhu, X.L., Hu, L.: The effect of Nd content on the electrochemical properties of low-Co La–Mg–Ni-based hydrogen storage alloys. J. Alloy. Compd. **458**, 357–362 (2008)
22. Jiang, L., Li, G.X., Xu, L.Q., Jiang, W.Q., Lan, Z.Q., Guo, J.: Effect of substituting Mn for Ni on the hydrogen storage and electrochemical properties of $ReNi_{2.6-x}Mn_xCo_{0.9}$ alloys. Int. J. Hydrog. Energy **35**, 204–209 (2010)
23. Denys, R.V., Riabov, B., Yartys, V.A., Delaplane, R.G., Sato, M.: Hydrogen storage properties and structure of $La_{1-x}Mg_x(Ni_{1-y}Mn_y)_3$ intermetallics and their hydrides. J. Alloy. Compd. **446–447**, 166–172 (2007)
24. Liu, Y.F., Pan, H.G., Gao, M.X., Li, R., Lei, Y.Q.: Effect of Co content on the structural and electrochemical properties of the $La_{0.7}Mg_{0.3}Ni_{3.4-x}Mn_{0.1}Co_x$ hydride alloys: I. The structure and hydrogen storage. J. Alloy. Compd. **376**, 296–303 (2004)
25. Liao, B., Lei, Y.Q., Chen, L.X., Lu, G.L., Pan, H.G., Wang, Q.D.: Effect of Co substitution for Ni on the structural and electrochemical properties of $La_2Mg(Ni_{1-x}Co_x)_9$(x = 0.1–0.5) hydrogen storage electrode alloys. Electrochim. Acta **50**, 1057–1063 (2004)
26. Liao, B., Lei, Y.Q., Chen, L.X., Lu, G.L., Pan, H.G., Wang, Q.D.: A study on the structure and electrochemical properties

of $La_2Mg(Ni_{0.95}M_{0.05})_9$ (M = Co, Mn, Fe, Al, Cu, Sn) hydrogen storage electrode alloys. J. Alloy. Compd. **376**, 186–195 (2004)
27. Liao, B., Lei, Y.Q., Chen, L.X., Lu, G.L., Pan, H.G., Wang, Q.D.: The effect of Al substitution for Ni on the structure and electrochemical properties of AB3-type $La_2Mg(Ni_{1-x}Al_x)_9$ (x = 0–0.05) alloys. J. Alloy. Compd. **404–406**, 665–668 (2005)
28. Liu, J.J., Han, S.M., Li, Y., Yang, S.Q., Zhang, L., Zhao, Y.M.: Effect of Al incorporation on the degradation in discharge capacity and electrochemical kinetics of La–Mg–Ni-based alloys with A_2B_7–type super-stacking structure. J. Alloy. Compd. **619**, 778–787 (2015)
29. Young, K., Ouchi, T., Wang, L., Wong, D.F.: The effects of Al substitution on the phase abundance, structure and electrochemical performance of $La_{0.7}Mg_{0.3}Ni_{2.8}Co_{0.5-x}Al_x$ (x = 0, 0.1,0.2) alloys. J. Power Sources **279**, 172–179 (2015)
30. Guzik, M.N., Lang, J.L., Huot, J., Sartori, S.: Effect of Al presence and synthesis method on phase composition of the hydrogen absorbing La–Mg–Ni-based compounds. Int. J. Hydrog. Energy **42**, 30135–30144 (2017)
31. Wang, B.P., Chen, Y.Z., Wang, L., Liu, Y.N.: Effect of annealing time on the structure and electrochemical properties of $La_{0.72}Nd_{0.08}Mg_{0.2}Ni_{3.4}Al_{0.1}$ hydrogen storage alloys. J. Alloy. Compd. **541**, 305–309 (2012)
32. Nwakwuo, C.C., Holm, T., Denys, R.V., Hu, W., Maehlen, J.P., Solberg, J.K., Yartys, V.A.: Effect of magnesium content and quenching rate on the phase structure and composition of rapidly solidified La_2MgNi_9 metal hydride battery electrode alloy. J. Alloy. Compd. **555**, 201–208 (2013)
33. Young, K., Chao, B., Bendersky, L.A., Wang, K.: $Ti_{12.5}Zr_{21}V_{10}Cr_{8.5}Mn_xCo_{1.5}Ni_{46.5-x}$ AB_2-type metal hydride alloys for electrochemical storage application: Part 2. Hydrogen storage and electrochemical properties. J. Power Sources **218**, 487–494 (2012)
34. Young, K., Ouch, T., Reichman, B., Koch, J., Fetcenko, M.A.: Effects of Mo additive on the structure and electrochemical properties of low-temperature AB_5 metal hydride alloys. J. Alloy. Compd. **509**, 3995–4001 (2011)
35. Young, K., Ouchi, T., Reichman, B., Koch, J., Fetcenko, M.A.: Improvement in the low-temperature performance of AB_5 metal hydride alloys by Fe-addition. J. Alloy. Compd. **509**, 7611–7617 (2011)
36. Young, K., Ouchi, T., Huang, B.: Effects of annealing and stoichiometry to (Nd, Mg)(Ni, Al)$_{3.5}$ metal hydride alloys. J. Power Sources **215**, 152–159 (2012)
37. Jiang, W.Q., Qin, C.S., Zhu, R.R., Guo, J.: Annealing effect on hydrogen storage property of Co-free $La_{1.8}Ti_{0.2}MgNi_{8.7}Al_{0.3}$ alloy. J. Alloy. Compd. **565**, 37–43 (2013)
38. Young, K., Ouchi, T., Huang, B., Reichman, B., Fetcenko, M.A.: Studies of copper as a modifier in C14-predominant AB_2 metal hydride alloys. J. Power Sources **204**, 205–212 (2012)
39. Miao, H., Pan, H.G., Zhang, S.C., Chen, N., Li, R., Gao, M.X.: Influences of Co substitution and annealing treatment on the structure and electrochemical properties of hydrogen storage alloys $La_{0.7}Mg_{0.3}Ni_{2.45-x}Co_{0.75+x}Mn_{0.1}Al_{0.2}$(x = 0,0.15,0.30). Int. J. Hydrog. Energy **32**, 3387–3394 (2007)
40. Kleperis, J., Wójcik, G., Czerwinski, A., Skowronski, J., Kopczyk, M., Beltowska-Brzezinska, M.: Electrochemical behavior of metal hydrides. J. Solid State Electrochem. **5**, 229–249 (2001)
41. Miao, H., Gao, M.X., Liu, Y.F., Zhu, D., Pan, H.G.: An improvement on cycling stability of Ti–V–Fe-based hydrogen storage alloys with Co substitution for Ni. J. Power Sources **184**, 627–632 (2008)
42. Liu, Y.F., Pan, H.G., Gao, M.X., Lei, Y.Q., Wang, Q.D.: Degradation Mechanism of the La–Mg–Ni-Based Metal Hydride Electrode $La_{0.7}Mg_{0.3}Ni_{3.4}Mn_{0.1}$. J. Electrochem. Soc. **152**, A1089–A1095 (2005)
43. Zhao, Y., Gao, M.X., Liu, Y.F., Huang, L., Pan, H.G.: The correlative effects of Al and Co on the structure and electrochemical properties of a La–Mg–Ni-based hydrogen storage electrode alloy. J. Alloy. Compd. **496**, 454–461 (2010)
44. Zhang, P., Liu, Y.N., Zhu, J.W., Wei, X.D., Yu, G.: Effect of Al and W substitution for Ni on the microstructure and electrochemical properties of $La_{1.3}CaMg_{0.7}Ni_{9-x}(Al_{0.5}W_{0.5})_x$ hydrogen storage alloys. Int. J. Hydrog. Energy **32**, 2488–2493 (2007)
45. Pan, H.G., Liu, Y.F., Gao, M.X., Lei, Y.Q., Wang, Q.D.: Electrochemical properties of the $La_{0.7}Mg_{0.3}Ni_{2.65-x}Mn_{0.1}Co_{0.75}Al_x$(x = 0–0.5) hydrogen storage alloy electrodes. J. Electrochem. Soc. **152**, A326–A332 (2005)
46. Li, R.F., Wan, J., Wang, F., Ding, C.P., Yu, R.H.: Effect of non-stoichiometry on microstructure and electrochemical performance of $La_{0.8}Gd_xMg_{0.2}Ni_{3.15}Co_{0.25}Al_{0.1}$ (x = 0–0.4) hydrogen storage alloys. J. Power Sources **301**, 229–236 (2016)
47. Tian, X., Wei, W., Duan, R.X., Zheng, X.Y., Zhang, H.W., Tegus, O., Li, X.G.: Preparation and electrochemical properties of $La_{0.70}Mg_xNi_{2.45}Co_{0.75}Al_{0.30}$ (x = 0, 0.30, 0.33, 0.36, 0.39) hydrogen storage alloys. J. Alloy. Compd. **672**, 104–109 (2016)